Smart Structures and Systems, *Vol. 14, No. 4 (2014) 569-594*
DOI: http://dx.doi.org/10.12989/sss.2014.14.4.569

Influence of sharp stiffness variations in damage evaluation using POD and GSM

M. Thiene[*1,2], U. Galvanetto[1, 2] and C. Surace[3]

[1]*Department of Industrial Engineering, University of Padova, via Marzolo 9, 35131 Padova, Italy*
[2]*Centre for Space Studies and Activities G. Colombo, University of Padova, via Venezia 15, 35131 Padova, Italy*
[3]*Department of Structural, Geotechnical and Building Engineering, Politecnico di Torino, corso Duca degli Abruzzi 24 – 10129 Turin, Italy*

(Received January 30, 2013, Revised August 20, 2013, Accepted October 19, 2013)

Abstract. Damage detection methods based on modal analysis have been widely studied in recent years. However the calculation of mode shapes in real structures can be time consuming and often requires dedicated software programmes. In the present paper the combined application of proper orthogonal decomposition and gapped smoothing method to structural damage detection is presented. The first is used to calculate the dynamic shapes of a damaged structural element using only the time response of the system while the second is used to derive a reference baseline to which compare the data coming from the damaged structure. Experimental verification is provided for a beam case while numerical analyses are conducted on plates. The introduction of a stiffener on a plate is investigated and a method to distinguish its influence from that of a defect is presented. Results highlight that the derivatives of the proper orthogonal modes are more effective damage indices than the modes themselves and that they can be used in damage detection when only data from the damaged structure are available. Furthermore the stiffened plate case shows how the simple use of the curvature is not sufficient when analysing complex components. The combined application of the two techniques provides a possible improvement in damage detection of typical aeronautical structures.

Keywords: damage detection; POD; GSM; stiffened panel; threshold approach

1. Introduction

In many engineering applications monitoring of structural components is crucial for the safety of both the structure and people. In recent years a large number of papers have addressed the problem of damage detection. Particular attention has been paid to composite materials that are widely used in the aeronautical field because they suffer various damage initiation and evolution mechanisms.

Commonly used non-destructive techniques (NDTs) are now considered reliable methods to verify the integrity of structures. However they can be applied only to a small portion of the structure, knowing a priori the position of possible damage. The variation of vibrational

∗Corresponding author, E-mail: marco.thiene.1@studenti.unipd.it

http://www.techno-press.org/?journal=sss&subpage=8 ISSN: 1738-1584 (Print), 1738-1991 (Online)

characteristics of structural components, as damage indicators at the global level, has been widely investigated. Change in natural frequencies, damping ratios and modal shapes have been considered as indices for damage evaluation (Doebling *et al*. 1998). Modal shapes, and in particular their curvatures, have the capability not only to detect the presence of damage but also to determine its position (Ratcliffe 1997). One of the greatest limitations of the use of vibrational methods is that they usually require the comparison between the current status of the structure and a known pristine condition. This step can be avoided if the shape of the damaged mode is smoothed with a polynomial. This approach has been presented by several authors and different interpolation techniques have been studied.

The gapped smoothing method (GSM) is one of the most applied techniques and good results were already presented for damage detection with mode shape curvatures (Ratcliffe and Bagaria 1998, Ratcliffe 2000, Hamey *et al*. 2004, Wu and Law 2004, Yoon *et al*. 2005, Qiao *et al*. 2007, Cao and Qiao 2009, Radzieński *et al*. 2011, Zhang *et al*. 2012). However these papers applied the method to simple cases like beams and plates in cantilevered and simply supported configurations. An application of the curvature as damage index to a more realistic structure was performed in conical shells, (Xiang *et al*. 2012),but in this case still a comparison with a pristine case was used. The basic concept of the GSM is that damage causes a variation in structural stiffness, which produces a sharp change in the curvature of modal shapes. This sharp variation can be smoothed by approximating the curvature with an interpolation, in order to obtain a baseline representative of the pristine status. Common structural elements in the aeronautical field however are not simple beams or plates. A typical example is a panel with stiffeners which increase its bending stiffness. It is apparent that stringers create much localised stiffness variations, which can hide variations caused by small amounts of damage. Obviously a smoothing technique such as the GSM would detect such sharp variations, as from a mathematical point of view they would not be easily distinguished from those due to the presence of a defect, and ambiguities in damage evaluation can arise.

In this paper the GSM will be applied in conjunction with the proper orthogonal decomposition (POD). In the following paragraphs this new methodology is first implemented experimentally onto a beam case. Then numerical analyses on a cantilever plate and on a stiffened panel are performed. The issues which arise due to the presence of the stringer are overcome with a different baseline computation and a threshold approach. The novel contributions of the present paper are:

- the application of GSM to the gradient and the curvature calculated on the POD generated data;
- the application of the method to a stiffened panel;
- the introduction of the different baseline computation and a threshold approach.

The basic ideas of Proper Orthogonal Decomposition and GSM are presented in sections 2 and 3. Their application to a lab experiment involving a cantilever beam is given in section 4; in section 5 a numerical application to a cantilever plate introduces the most innovative part of the paper about stiffened plates (section 6) and the threshold approach (section 7). After several remarks on noise (section 9), excitation frequency (section 10) and number of sensors (section 11) the conclusions bring the paper to the end.

2. Proper orthogonal decomposition: overview

Proper orthogonal decomposition (POD) was used by several authors in different disciplines as fluid dynamics (Holmes *et al*. 1998), chemical processes (Graham and Kevrekidis 1996), medicine (Bayly *et al*. 1995) and others. In structural dynamics it was first applied in the early 1990s for the determination of low dimensional models of distributed systems (Fitzsimons and Rui 1993), (Cusumano *et al*. 1994). The method consists on a projection of data from a highly dimensional space to a space of lower dimension, keeping most of the information of the original system (Kerschen and Golinval 2002). The method can be described subdividing it in different parts:

- Acquisition of data of a vibrating structure over a certain period of time T. All the samples must be uniformly distributed in time
- Set up of a matrix V with dimensions $N{\times}M$ where N is the number of samples and M is the number of sensors. Each row represents a snapshot of the system at a certain time t_i while each column represents the time history of one point over the acquisition time T, Eq. (1)

$$\mathbf{V} = \begin{bmatrix} v_1(t_1) & v_2(t_1) & v_3(t_1) & \dots & v_M(t_1) \\ v_1(t_2) & v_2(t_2) & v_3(t_2) & \dots & v_M(t_2) \\ \vdots & \vdots & \vdots & \ddots & \vdots \\ v_1(t_N) & v_2(t_N) & v_3(t_N) & \dots & v_M(t_N) \end{bmatrix} \tag{1}$$

- Subtracting the mean value from each column of matrix V, Eq. (2)

$$\mathbf{U} = \mathbf{V} - \frac{1}{N}\begin{bmatrix} \sum_{t=1}^{N} v_1(t_t) & \sum_{t=1}^{N} v_2(t_t) & \sum_{t=1}^{N} v_3(t_t) & \dots & \sum_{t=1}^{N} v_M(t_t) \\ \sum_{t=1}^{N} v_1(t_t) & \sum_{t=1}^{N} v_2(t_t) & \sum_{t=1}^{N} v_3(t_t) & \dots & \sum_{t=1}^{N} v_M(t_t) \\ \vdots & \vdots & \vdots & \ddots & \vdots \\ \sum_{t=1}^{N} v_1(t_t) & \sum_{t=1}^{N} v_2(t_t) & \sum_{t=1}^{N} v_3(t_t) & \dots & \sum_{t=1}^{N} v_M(t_t) \end{bmatrix} \tag{2}$$

- Building of the spatial correlation matrix R as shown in Eq. (3)

$$\mathbf{R} = \frac{1}{N}\mathbf{U}^T\mathbf{U} \tag{3}$$

R results to be real, square and symmetric, with dimensions $M{\times}M$. Its eigen-values are called proper orthogonal values (POVs) while its eigen-vectors proper orthogonal modes (POMs). It was shown in (Feeny and Kappagantu 1998) that POMs are strictly related to the Linear Natural Modes (LNMs) of a vibrating structure with uniform mass distribution while each POV represents the energy associated with the corresponding POM. For a forced motion the POMs can be used to describe the deformed configuration using fewer modes than in the superposition of LNMs approach (Kerschen *et al*. 2005). The relationship between LNMs and POMs was also recognized for randomly excited vibrations(Feeny and Liang 2003, Hensman *et al*. 2011). The number of POMs that can be evaluated is equal to the number of sensors *M,* and therefore only a sufficiently high number *M* will provide an accurate enough description of the dynamic behaviour of the structure, but the key factor is that for damage detection it is not necessary to study all the POMs. An energetic criterion is used to determine the number of POMs needed to describe the dynamics of the component. The energy associated with a POM is defined by its POV and it is assumed that the number of POMs required to give an accurate description of the dynamics of the structure is associated to a number j defined by the following equation

$$j : \frac{\sum_{i=1}^{j} \lambda_i}{\sum_{i=1}^{M} \lambda_i} \geq 0.999 \tag{4}$$

Usually very few POMs are required to satisfy Eq. (4), sometimes even just one.

An application of POD as damage detection method was performed both numerically and experimentally (Galvanetto and Violaris 2007, Galvanetto *et al*. 2008). In those papers the damage index was computed comparing POMs belonging to a damaged case to the ones evaluated on an undamaged beam. Results showed that the difference between the two cases presented a sharp variation in correspondence to the sensors close to the damage. One of the greatest issues concerning this type of analysis is that a pristine case to which compare actual data is not always available, especially in real cases. For this reason a method capable to detect damage without referring to a reference case is preferable. One possibility is to smooth the shape of the POM, in order to delete any sharp variation. This new smoothed POM is used as reference case; the evaluation of possible damage is hence performed comparing the real POM with the smoothed one. A first attempt to apply the POD without referring to a pristine case was performed in (Galvanetto, *et al*. 2007). The system under examination was a cantilever beam with a saw cut close to half of its length. Applications of the POD to bidimensional elements can be found in (Shane and Jha 2011, Thiene *et al*. 2013).

3. Derivatives of mode shapes and gapped smoothing method

Previous works on damage detection using modal shape data demonstrated how the damage index can be enhanced using derivatives of mode shapes. In particular their curvatures are more effective in localizing a possible damage. For a beam case this is easily demonstrated as the curvature is directly related to its bending stiffness (Cao and Qiao 2009)

$$-\frac{M}{EI} = \varphi''(x) \approx \frac{\varphi(x-h) - 2\varphi(x) + \varphi(x+h)}{h^2} \tag{5}$$

When working with a bidimensional element, the above equation can be modified as follows

$$\varphi''(x, y) = \frac{\varphi(i-1, j) - 2\varphi(i, j) + \varphi(i+1, j)}{h_x^2} + \frac{\varphi(i, j-1) - 2\varphi(i, j) + \varphi(i, j+1)}{h_y^2} \tag{6}$$

In Eq. (6) $\varphi(i,j)$ are the components of the relevant POMs and the meaning of all the indices can be found in Fig. 1(a)). Although the curvature of mode shapes has been widely recognised as a powerful tool to reveal the presence of damage, (Ratcliffe 2000, Hamey *et al*. 2004, Wu and Law 2004, Qiao *et al*. 2007, Xiang *et al*. 2012, Zhang *et al*. 2012), it can be successfully applied only when a sufficient number of grid points, i.e. sensors on the monitored structure, is available. This is due to the formulation of Eq. (5). As it consists on a central difference method, it performs better when the points considered in the equation are close to each other. An alternative damage index is the gradient of the POM. Even if its relationship with the bending stiffness of a beam is not so straightforward, it has the advantage of highlighting any POM variation. For cases in which the number of sensors is limited, as the one shown in the following section, it should be preferred to the curvature. The gradient, for a discrete case, can be calculated as

$$\varphi'(x) = \frac{\varphi(x+h) - \varphi(x)}{h} \tag{7}$$

The above formulation reports a possible improvement in damage evaluation. However it still does not overcome the problem related to the necessity of a pristine case to which compare the available data (gradient or curvature of POMs). To solve this issue, an artificial reference case can be derived by smoothing available data; this is the principle at the base of the gapped smoothing method (Ratcliffe and Bagaria 1998).

Starting from the curvature of the damaged component, the interpolated curvature can be calculated. For a beam case a simple cubic spline can be used

$$\varphi''(x) = a_0 + a_1 x + a_2 x^2 + a_3 x^3 \tag{8}$$

At each grid point the smoothed value of the parameter under examination is evaluated using values of the adjacent grid points. In this way a sharp variation, which affects only few nodes, is smoothed as shown in Fig. 2.

For a bidimensional case an extension in two variables (x, y) of Eq. (8) can be derived (Battipede *et al*. 2001, Wu and Law 2004, Gherlone *et al*. 2005). However that equation suffers from bad conditioning at the edges of the structure. An improved version of the interpolation was proposed in (Yoon *et al*. 2005). This approach can take into account the fact that, depending on the position of the point, the number of neighbouring points which can be used in the interpolation is different as shown in Fig. 1(b)). In the present paper the above approach is applied when dealing with the plate examples, for the detailed formulation the reader can refer to the mentioned reference.

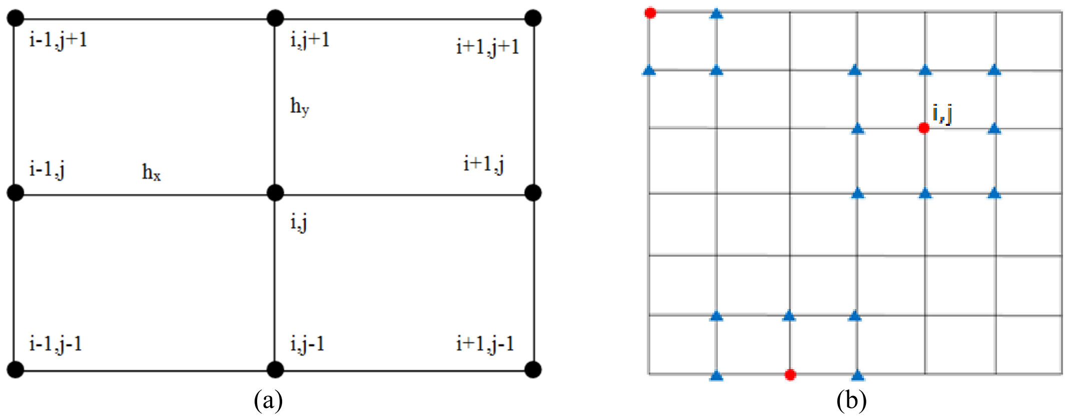

Fig. 1 (a) Description of the indices for the curvature calculation and (b) Neighbouring points for 2d GSM

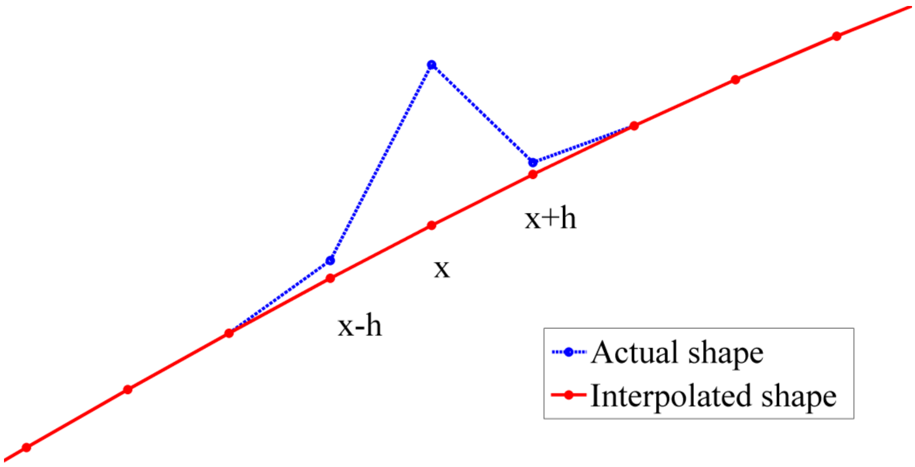

Fig. 2 Example of smoothing of data shape

4. Experimental verification on a cantilever beam

The experimental case under examination is described in (Galvanetto *et al*. 2007, Galvanetto *et al*. 2008). In these papers the verification was done first with the POD applied both to a pristine and damaged beam (classic POD), then using only damaged data. In particular in this last case the smoothing technique was applied to the main POM. A fitting of the actual grid was performed in order to obtain a better result with the smoothing technique. The main contribution of the present section is the application of the damage detection algorithm to the gradient of the POMs without increasing the density of the grid. The system under examination is a cantilever beam with length L=600 mm and square cross section 20x20 mm^2. The material is steel, AISI 1030. 13 accelerometers, from x=20 mm till x=500 mm with 40 mm spacing, were used to acquire the response of the beam under sinusoidal excitation at 40 Hz, produced by a shaker placed close to its free end. A saw cut, 1 mm in depth, was produced at x = 230mm, between sensor 6 (x=220 mm) and sensor 7 (x=260 mm). The POD is applied and then the gradient of the POMs calculated. In particular the first two POMs are considered in the damage evaluation. The use of the curvature could not be accomplished as the number of sensor is too small and the grid space between them is too large (this is a typical issue when working with the curvature).

The damage index shown along the vertical axes of Fig. 3 is the difference between the value of φ' given by Eq. (7) and its interpolated value given by the application of Eq. (8). Fig. 3 shows that it is possible to locate the saw cut using only data coming from the damaged beam. It is interesting to notice how the damage index, which was calculated differentiating the actual gradient of the POM and the smoothed one, is higher when the gradient of the second POM is considered.

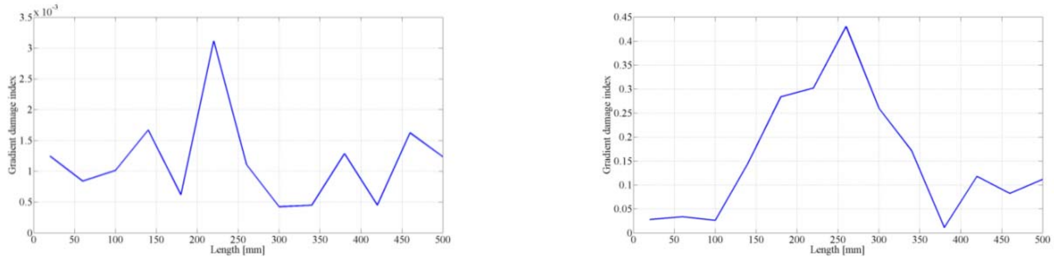

(a) (b)

Fig. 3 Gradient damage index for the experimental beam analysis. (a) 1st POM gradient and (b) 2nd POM gradient

5. Cantilever plate

Numerical verifications of the methodology presented in section 2 and 3 have been conducted on different structural elements. GSM applied to curvature of modal shapes was already successfully applied, as already explained in section 3. However the application of GSM to the curvature of the proper orthogonal modes has not been investigated yet. The first example which is proposed is a cantilever plate made of composite plies. The damage introduced is a delamination between different layers of the layup, three cases are considered with delamination at the following interfaces: 4^{th}-5^{th}, 5^{th}-6^{th}, 7^{th}-8^{th}. Two positions of damage in the plane are considered, as shown in Fig. 4. All information about the plate can be found in Table 1. The plate is loaded with a harmonic force with frequency close to its first natural one, applied close to one corner. This approach is commonly used in damage detection with POD. 117 points on the mesh grid are used as outputs. Thanks to this high number of outputs, in this case the difference between actual and smoothed curvatures was used as damage indicator. The smoothed curvature can be considered representative of an ideal pristine case, as already stated in Section 3 and in the references provided. The analysis highlights how the curvature of the POMs is capable to detect a possible damage without a comparison to a pristine case, as no data belonging to a real undamaged case were considered when computing the damage index. Fig. 5 shows the result for damage in position 1 while in Fig. 6 a comparison between different damage indices is given. In particular some points can be noted, for the cantilever plate:

- The technique is more sensitive to damage closer to the fixed edge
- Delamination in the inner layers causes a higher value of the damage index

Table 1 Mechanical properties and geometrical characteristics of the plate

E11=140 GPa	E22=9.7 GPa	G12=5 GPa	G13=5 Gpa
G23=5 Gpa	ν=0.3	ρ=1715 kg/m^3	Boundary condition: cantilever
Dimensions: 300x400x2.7 mm^3		Layup: 8 layers [0°/45°/-45°/90°]s	
Position of damage 1		Position of damage 2	
X=105 mm	Y=85 mm	X=105 mm	Y=160 mm

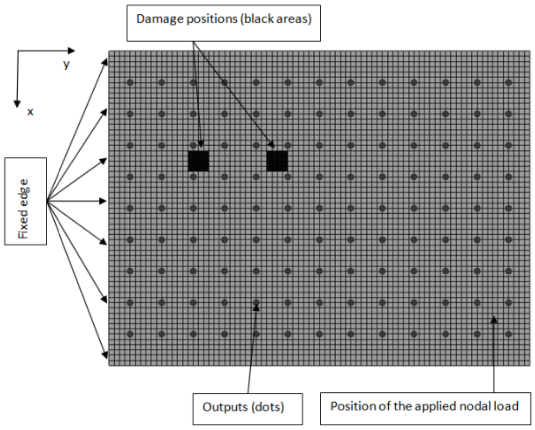

Fig. 4 Cantilever plate

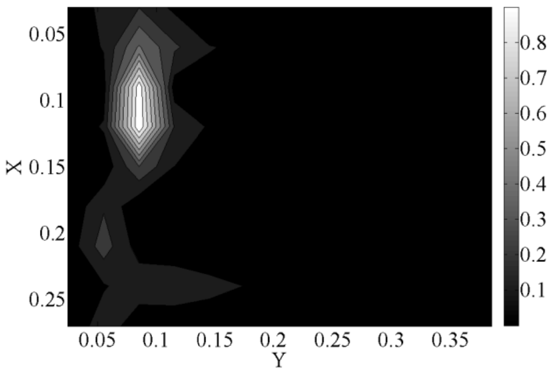

Fig. 5 Damage index for position 1, cantilever plate. Dimensions of the axes in m

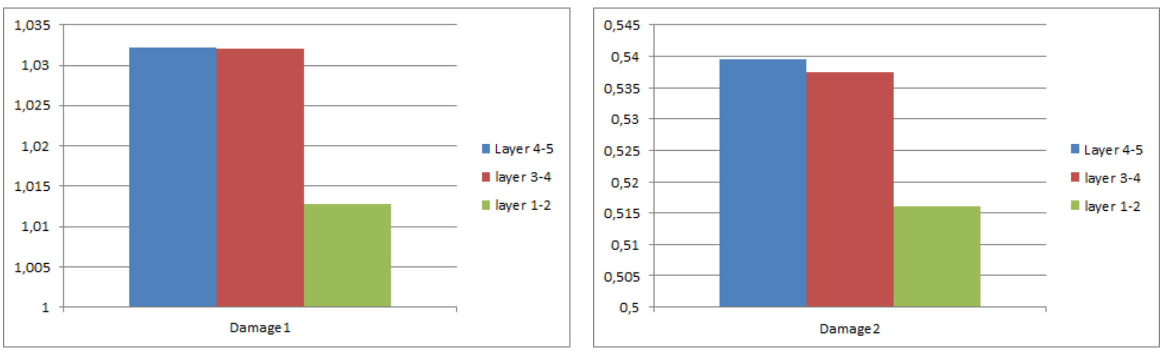

(a) (b)

Fig. 6 Variation of the damage index along the thickness. (a) Position 1 and (b) Position 2

6. Stiffened plate

In the previous sections it was shown how GSM coupled with POD, applied to a simple component, is able to locate one defect. However in that ideal case the only contribution to the change in the local stiffness of the plate was due to the presence of damage. Plates commonly used in the aeronautical field are usually stiffened with stringers. These obviously create a sharp change in the local stiffness, which usually is much higher than the one produced by low level damage. For this reason it can be useful to study the effect of this kind of structural elements when a technique such GSM is applied to damage detection. The model which is analysed is a composite plate, pinned at all the edges, with a stringer. Both the plate and the stringer are made of composite layers. The model of the plate can be seen in Fig. 7(a)) while in Fig. 7(b)) a sketch of the stringer is presented. The material properties and other information on the system can be found in Table 2. Different positions and entities of damage are considered. One type of damage is the softening of a local area in the plate, shown in black in Fig. 8. Two levels of this type of damage are considered: softening of the two innermost layers and softening of all the layers, both of 90% of the original elastic moduli. Another typology of defect is a local debonding between the stiffener and the plate. Two different sizes for this debonding are considered: small, black area in Fig. 8, and big, area enclosed in the black rectangle in Fig. 8. The external load is distributed on the free flange of the stiffener in the direction normal to the plane of the plate. Intensity and frequency of the load are 50 kPa-230 Hz. An analysis with a point load applied to the top of the plate, with the same frequency, was also conducted but the results were not as satisfactory as those of the present case. Before presenting the result of the analysis it is important to highlight the two main features of the structure: the presence of the stringer and the support boundary condition which is applied to all the edges of the plate and not just to one as in the cantilever case.

Numerical results show that the influence of the stringer is strong, hiding in most of the cases the presence of the defect. In particular in the case of low level damage it was not possible to have a clear evidence of the softening in the plate. For the high level damage it resulted that damage at position 2 was the easiest to locate whereas position 1, Fig. 8, and position 3 weren't clearly identifiable. Also for the deboning case it was found that the smaller damage was difficult to detect. However the deboning was easier to identify than the softening at that position. In all cases, both for the classic POD and the GSM, position 2 was the one that led to the highest value of the damage index, as indicated in Table 3. Finally it is worth to observe that in this case, with boundary conditions applied to all edges, the GSM does not seem to work better when the damage is close to the constraint, as in the case of the cantilever plate.

Table 2 Mechanical properties for the stiffened panel case

E11=150.15 GPa	E22=8.35 GPa	G12=4.2 GPa	G13=4.2 Gpa
G23=4.2 Gpa	ν=0.27	ρ=2100 kg/m^3	Boundary condition: 4 edges pinned
Plate dimensions: 300x400x2 mm^3		Layup (plate and stringer): 8 layers [0°/45°/-45°/90°]s	
Damage 1		Damage 2	
X=240 mm	Y=320 mm	X=230 mm	Y=80 mm

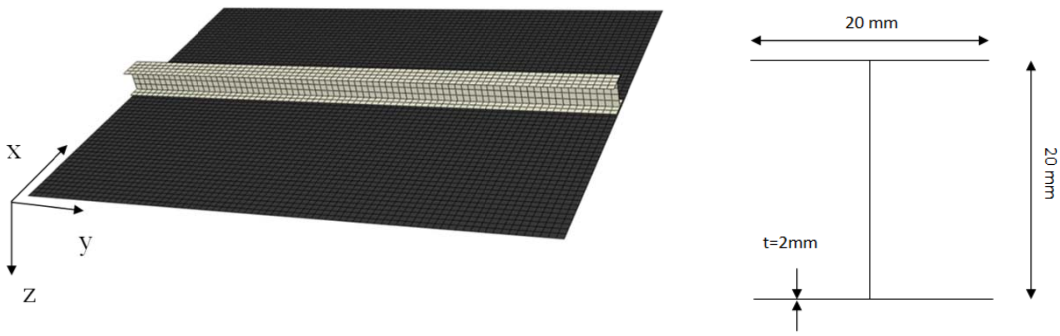

(a) (b)

Fig. 7 (a) 3D view of the stiffened panel and (b) Sketch of the stringer

Table 3 Normalised damage indices for the high level damage cases

Damage position	1	2	3	Debonding
Classic POD	0,661645	1	1,90E-01	0,667553
POD + GSM	0,615102	1	0,556338	0,838576

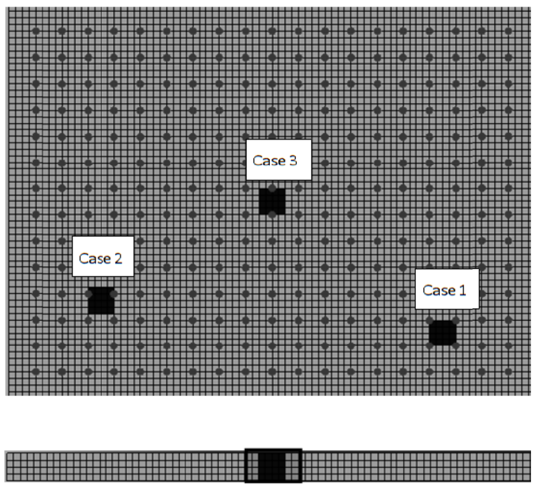

Fig. 8 Stiffened panel with damage positions

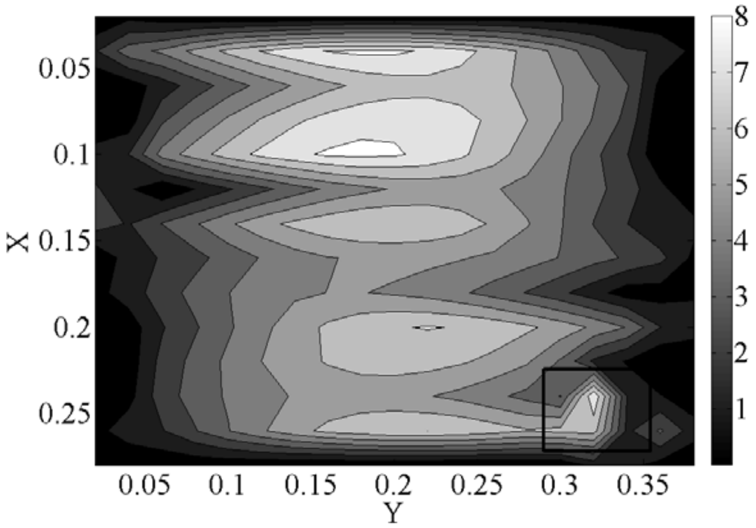

Fig. 9 Damage index evaluated with the GSM for Case 1 high level. The black rectangle shows the damage position

7. Threshold approach

In the previous paragraph it has been shown that the simple GSM coupled with POD and applied to a stiffened plate could not locate the damage since the stiffener creates a sharp change in the curvature which can conceal the effect of the defect. One potential way of avoiding this problem is studied in this paragraph.

This procedure could be applicable in cases in which the structure comprises a number of panels which have nominally the same geometrical and mechanical characteristics (as would occur, for example, if manufactured on a production line), as well as on a single panel which operates under different environmental conditions.

The first consideration concerns the opportunity to create a baseline from a single measurement on each individual panel. During a single data acquisition different sources of noise can be encountered together with other causes of temporary stiffness changes such as a variation in temperature or humidity. In this situation it can be useful to calculate a baseline from different sets. Before describing the procedure applied in this study, it is appropriate to mention that similar considerations were used in a damage detection application with a different interpolation approach (Limongelli 2010, Limongelli 2011).

An average of different acquisitions, all of them with different small local discontinuities due to different causes, can smooth these variations while maintaining all the common features. These can then be deleted when a comparison with a damaged case is considered. In the case under examination, the common feature which must be deleted in the damage evaluation is the stringer, while damage which was introduced is considered as possible stiffness change. In this way a new baseline is created to which each single damaged case is then compared to create an Improved Damage Index (IDI). This IDI is then compared to a chosen threshold, in order to set to zero the IDI values at all the grid points where it doesn't overcome a certain value.

The step by step procedure is as follows:

1. Application of the POD plus GSM approach to all the damaged cases under examination. In this way several different damage indices can be calculated. All of them share the contribution of the stringer.
2. Average all the damage indices calculated, in order to find a baseline which takes into account different conditions of the plate, not just a hypothetic undamaged status. With this step the contribution of the different damages is weakened while the influence of the stiffener is still present.
3. Calculate the damage index for a single case and compare it with the baseline, defining the IDI.
4. Define a threshold, if the result obtained with the previous step at each point is lower than the threshold, set it to zero (modified IDI).

The most challenging aspect of this approach is to find a threshold which is valid for most of the cases. Obviously it should be able to highlight the presence of damage without deleting even its contribution. For all the low level damage cases this approach results to be impractical, as the contribution of the stiffener is still too high to find the defect. Nevertheless it must be noted that the level of damage in those cases is low and that the baseline is computed considering also the high level damage cases. However for certain cases, damage 1 and 2 high level and big debonding area, the method provides good results. After the IDI has been defined in point 3, its absolute value was considered. The mean M and standard deviation S were then calculated and the threshold was calculated as

$$threshold = M + \alpha * S \tag{9}$$

Where α is a parameter which can be adjusted in order to suit most of the cases. In this case it was chosen equal to 5.5. This empirical value was appropriate for the three cases mentioned above. From Fig. 10(a)) it is clear how the IDI for case 1 high level presents the highest value close to position 1, but some other peaks are present. After the threshold approach all these heights are deleted and only the damage contribution remains, Fig. 10(b)). The results for the other two cases are presented in Fig. 11.

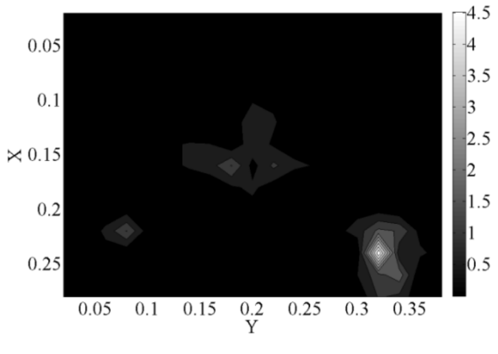

(a)

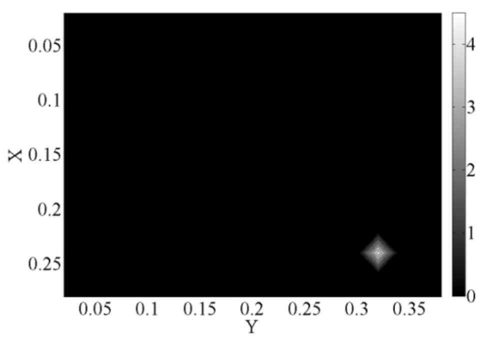

(b)

Fig. 10 (a) IDI for Case 1 high level and (b) IDI after threshold

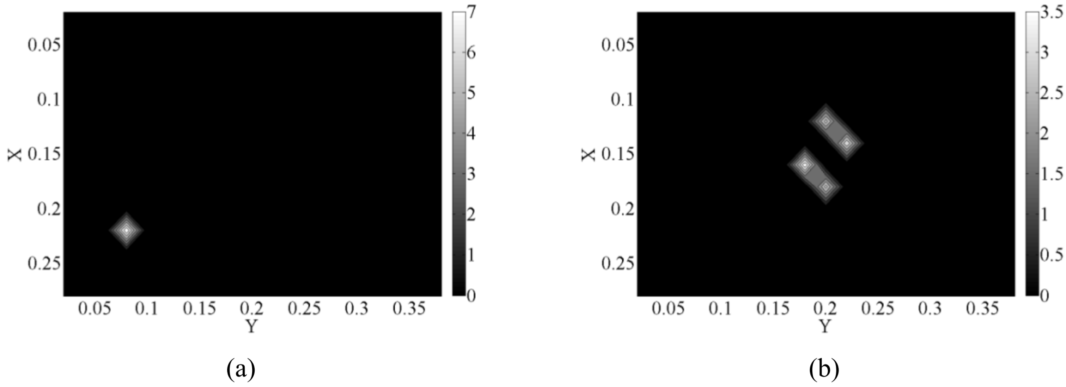

Fig. 11 Modified IDI. (a) Case 2 high level and (b) Big debonding

8. Remarks on the applicability of the proposed method

The case which has just been presented is representative of a typical stiffened panel which can be used for aeronautical applications. The algorithm proposed required several data which can be considered as training on the system. In this case, different damage configurations were used to create a baseline to which compare a possible damage scenario. A possible criticism about this could be the lack of generality of the method due to the definition of the threshold. This obviously depends on the single case and on the level of damage which is considered critical. However this type of specificity is something which lies in many damage detection algorithms, especially when complex structures are investigated. A possible example is given by the application of neural networks in SHM (Worden and Staszewski 2000, Zapico *et al*. 2003, Giurgiutiu 2008, De Stefano *et al*. 2011, Ghajari *et al*. 2012, Sharif-Khodaei *et al*. 2012, Ghajari *et al*. 2013). Although the algorithm underneath neural networks can be considered general, as it can be applied to many problems, like damage detection, aerodynamics, economy etc., every time the network must be trained with specific information, which is typical of the single case under exam. Finally it must be underlined that the only information required to perform the proposed algorithm is the dynamics of the system and the position of the sensors.

In real cases the baseline reference should be generated with several acquisitions of the dynamics of the panel under exam in different conditions. These can be, for example, temporary variations of boundary conditions (i.e., loosening of one bolt) or local variation of temperature (i.e., hot spots). A possible application can be connected to a reliable manufacturing process, in which the presence of faulty panels can be verified before they become available on the market. This can be particularly important for composite panels, which can present defects even during the manufacturing process. It is clear that most of these acquisitions should be recorded before the current damage is introduced in the structure, which is actually what is expected in the two applications mentioned above.

To prove the capability of the method in following sections the effect of noise and load frequency are investigated. Results will show that the method can locate damage also when these effects are included in the analysis.

9. Influence of noise

The presence of noise in the data can have an important influence on the performance of damage detection techniques. It can hide the effects of damage, as well as produce “false positive” cases. Mode based damage detection is affected by the level of noise present in data, and each mode can manifest different sensitivities towards it (Cavalini Jr. *et al*. 2008). Recently a thorough study on the effect of noise in the dynamics evaluation of systems was performed (Bentahar *et al*. 2013). In that case the nonlinearity of the system’s response was monitored and it was highlighted that noise level can modify the threshold at which the nonlinear effects, which can be easily referred as local damage, become relevant. Furthermore it was highlighted that the excitation frequency for the system should be close to its first natural one, in order to optimize the determination of the monitored feature.

Also POD can be affected by the presence of noise. The problem was already considered in (Galvanetto and Violaris 2007). In that case, however, still a comparison between a pristine and a damaged case was performed. A preliminary investigation of a probabilistic POD for noise reduction is given in (Hensman *et al*. 2010). The application of the curvature of mode shapes in damage detection further stresses the influence of noise in data. An important study on this topic was conducted on a cantilever beam (Cao and Qiao 2009). It was demonstrated that, even when the mode shape of a beam is not evidently affected by noise, its curvature can be completely corrupted, preventing not only the detection of damage, but also a correct representation of the curvature itself. The method proposed to overcome the problem was the application of a modified Laplacian operator, which applied Eq. (5) using bigger steps in between grid points ($2h$, $3h$,…). An extension of this study using the POD applied to bidimensional elements can be found in (Thiene *et al*. 2014).

In the present study an analysis similar to the one presented in section 7 was performed adding white Gaussian noise to the data used to compute the POD. In particular two levels of noise are presented here. The command *awgn* available in Matlab was used with levels of signal to noise ratio, SNR, equal to 40 and 20. Higher values of SNR (100, 80 and 60) provided results comparable to the uncorrupted case; hence they are not shown in this paper. An example of the standard damage index with SNR equal to 40 is given in Fig. 12 where damage cannot be detected. The application of the IDI and threshold approach revealed that the influence of noise can be overcome, as the averaging technique is able to remove noise effects. The explanation of this can be found on the nature itself of the white Gaussian noise, which has a flat power spectral density, normal distribution, zero mean and finite variance.

The noise is hence expected to corrupt the dynamic response of the plate with a zero mean, and a finite variance σ. This obviously affects the POMs; furthermore its effects are even amplified when a double differentiation is applied. The application of the threshold can therefore delete also the influence of this variation, if its level is below the threshold itself. The value of the variation is determined from the given SNR (Matworks 2012). The corruption of the signal is obtained with Eqs. (10)-(12)

$$noise\_level = 10^{-\frac{SNR}{10}} \tag{10}$$

$$noise = \sqrt{noise\_level * rand} \tag{11}$$

$$data\_noise = data + noise \tag{12}$$

Where the variable *randn* in Eq. (11) refers to a random number.

Results for the first position damage case are presented in Figs. 13-15. The same results for the first and second damage cases were obtained even after the addition of noise while for the big debonding the chosen value of alpha resulted to be appropriate only for the case of SNR equal to 40. The difference between the case without noise, in which the same value of alpha was used for these sets, and this case with noise in which it could not be used successfully, is explained with the variance of the noise, which in this case overcomes the threshold level. A summary of the results obtained with the addition of noise can be found in Table 4.

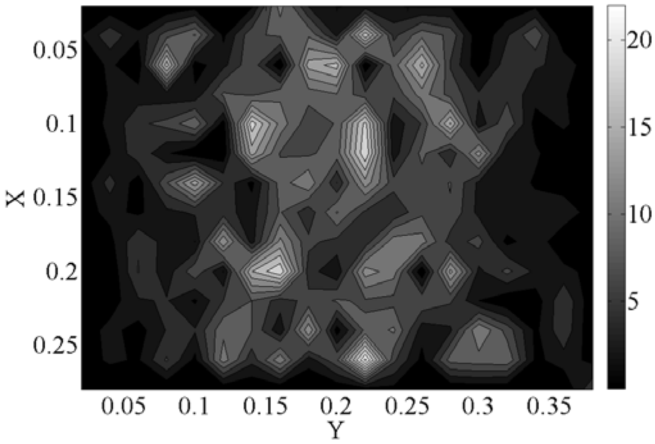

Fig. 12 Case 1, standard index, SNR 40. The noise hides the damage

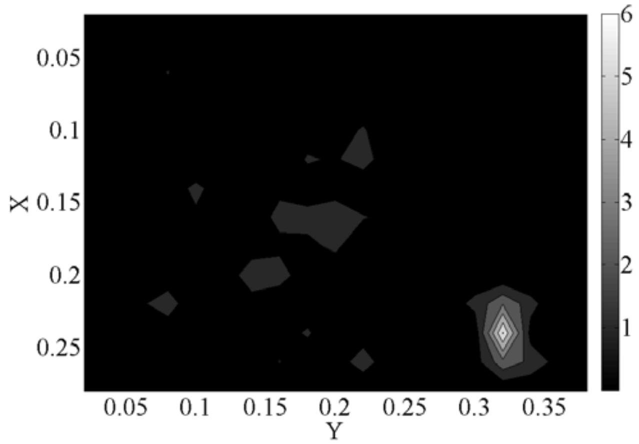

Fig. 13 Case 1, IDI SNR 40. The damage is clearly identified

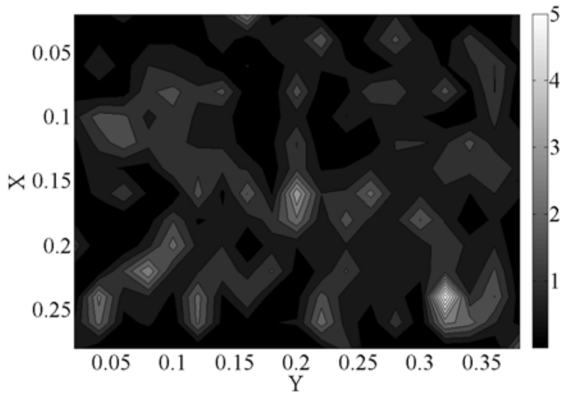

Fig. 14 Case 1, IDI SNR 20.The damage is identified

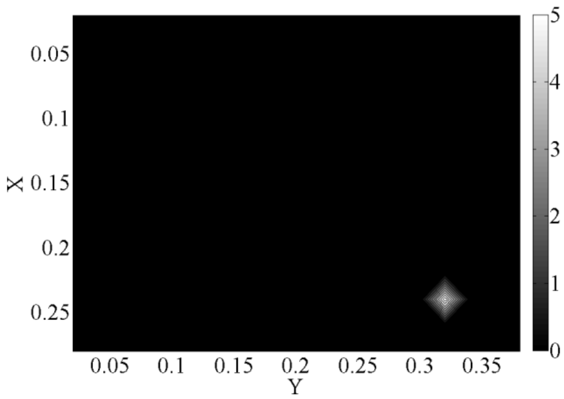

Fig. 15 Case 1, modified IDI SNR 20.The damage is clearly identified

Table 4 Summary of the results obtained after the addition of noise

Case	Noise level SNR	
	40	20
Damage 1high	detected	detected
Damage 2 high	detected	detected
Damage 3 high	missed	missed
Small debonding	missed	missed
Big debonding	detected	missed

10. Modification of the load frequency

In this section, in order to study the influence of the load frequency, the approach described in the previous paragraph was applied to data obtained from the same system under a harmonic load with frequency equal to 100 Hz. In this situation the dynamics of the system captured by the POM is different but the method should still be able to identify possible damage, as previous studies confirmed (Galvanetto *et al*. 2007, Galvanetto and Violaris 2007). The reason why this study is performed can be found in Appendix 1. An example for the big debonding case, after corrupting data with SNR equal to 40 is presented in Fig. 16. In general it was found that the amplitude of the modified IDI was lower than in the case in which the frequency was higher, and that the number of missed detection increased. This can be due to a lower level of the system's response, as in the first case the frequency was close to the first natural frequency of the system, but also to the considerations presented in the appendix, which highlights that a variation of stiffness in a system can produce different effects in its mode shapes (as already mentioned, the POMs of a system are related to its LNMs).Those results can therefore be extended to the present application. The fact that the calculated damage indices change with the frequency is in accordance to what proposed in the appendix.

11. Considerations about the number of sensors

In most cases, the number of sensors needed to perform a reliable damage detection using modal data can be high. This is due to the fact that a correct determination of modal shapes and hence curvatures, needs a fine grid, in order to describe properly the dynamic behavior of the system. This is particularly true for a two-dimensional case. This limitation can be overcome employing advanced measurement instrumentation, such as SLV, capable of acquiring data at a large number of observation points. Details on this topic can be found in Appendix 2.

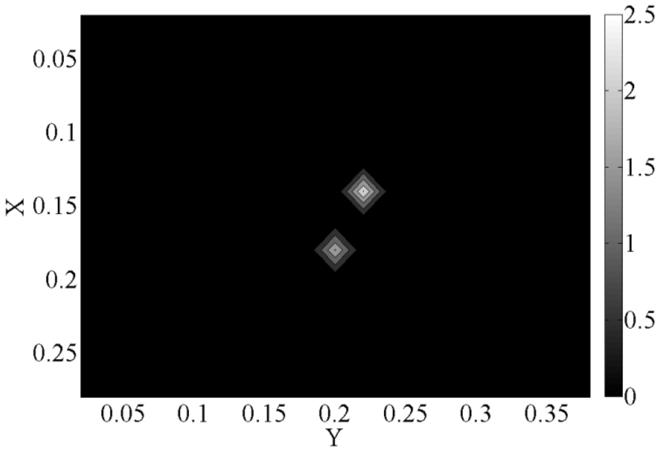

Fig. 16 Big debonding 100 Hz, modified IDI, SNR=40

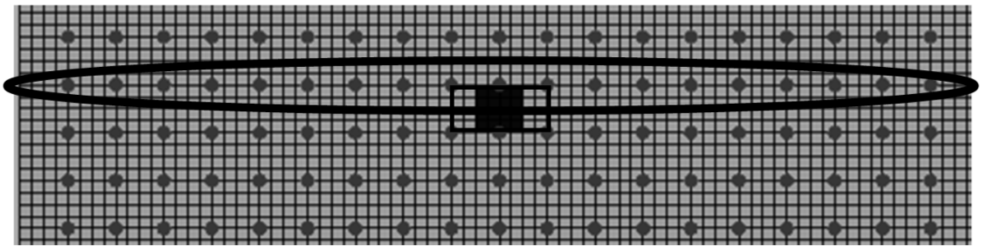

Fig. 17 Nodes used to perform the POD

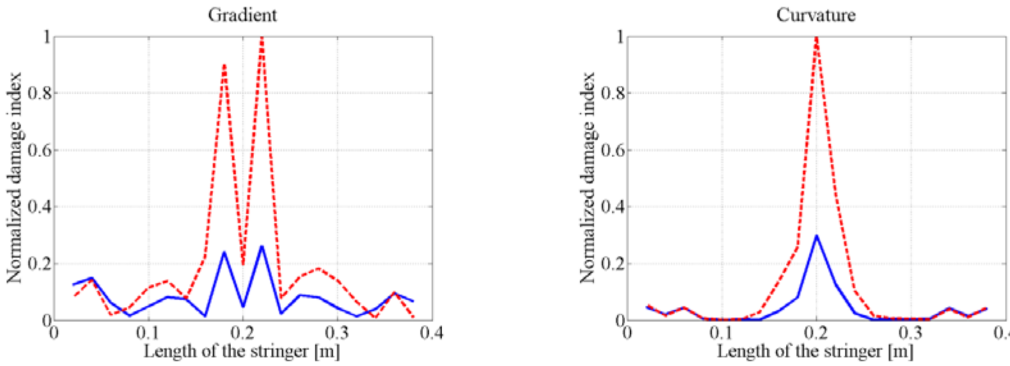

(a) (b)

Fig. 18 Normalized damage index with 19 outputs. The solid lines refer to small debonding while the dashedlines to the big debonding. (a) Gradient damage index and (b) Curvature damage index. Damage is correctly located

An example regarding this issue is given in section 4 in which the curvature could not be calculated accurately from experimental data due to the excessively coarse grid of the sensors. In the stiffened plate case under examination a 50% reduction of the number of outputs prevented the location of the damage. A more accurate analysis of their location with respect to that of damage could be useful to determine the sensitivity of the method to sensor density and location. However it is worth to notice that the determination of a possible debonding between plate and stringer doesn't necessarily need to be evaluated using data from a bi-dimensional grid. As the part of the system which is interested by this particular failure is narrow, only the dynamic of the plate over the stringer can be considered. In this section the POD plus GSM approach is applied using data only from sensors placed over the stringer. In particular the 19 nodes encircled by the line in Fig. 17 were considered; the full black square represents the small debonding while the black rectangle the big debonding. In Fig. 18 it is possible to see the results obtained for the two debonding cases using 19 outputs. The results were normalized in order to show the increase in the damage index when the debonding size was wider. Analyses with a smaller number of sensors were conducted in order to study the capability of this approach to locate the debonding also with fewer data. In particular two cases are shown: one in which 10 sensors were used (every other node from the first to the last in Fig. 17 and one in which 9 sensors were used (every other node from the second to the last but one in Fig. 17). The results indicate that for the main POM it is difficult to locate the damage. However using the second POM to perform the GSM the localization provides better results. This is also consistent with what found in section 4. The damage indices calculated from the gradient of the second POM are shown in Figs. 19 and 18(a), Figs. 19(a) and 19(b) present the same behavior of the damage index in proximity to the debonding. Two consecutive peaks are present close to the damage. However in the fewer node cases a spurious peak is also present at one node close to the boundary.

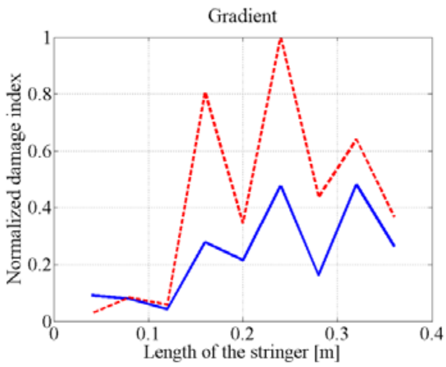

(a)

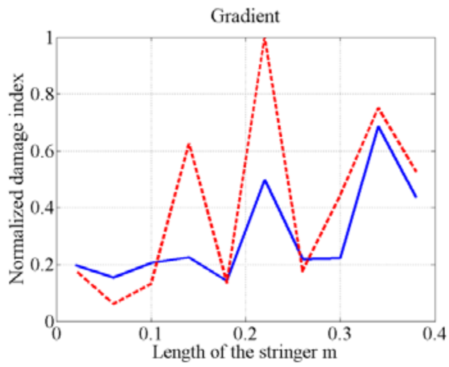

(b)

Fig. 19 Normalized damage index using the gradient of the second POM. The solid lines refer small debonding while the dashedlines to the big debonding. (a) 9 nodes case and (b) 10 nodes case

12. Conclusions

The present paper investigates the possibility to use derivatives of dynamic modes of a structure, computed by means of the proper orthogonal decomposition, to locate damage. The application of the gapped smoothing method to a damaged structure has been investigated in three cases: first with an experimental verification on a cantilever beam, then with a numerical analysis on a cantilever plate and finally on a stiffened panel. It was confirmed that for simple structures the use of gradient or curvature, combined with the GSM, is capable to locate damage. When the structure presents sharp changes in stiffness, due for example to the presence of a stringer, further numerical manipulation is required in order to remove the contribution of the stiffener to the curvature change. A new threshold approach has been proposed which, in certain cases, successfully distinguishes between damage and stiffener contribution. Moreover a possible solution for the determination of debonding between plate and stringer has been proposed, using only a small number of sensors to perform the analysis. In such a way this paper can extend the capabilities of damage detection techniques based only on data coming from damaged structures. In particular mode shapes usually require specific software programs to be evaluated whereas only the dynamic response of a structure is required to obtain its proper orthogonal modes. It is worth to observe that only the accelerations and the location of the sensors were used in the analysis. The material properties and the type of boundary conditions, although important for the final results as they can influence the level of the damage index, do not require any particular consideration or modeling when performing the POD and the GSM.

Aknowledgements

This research was partially supported by the Italian Ministry of Education, University and Research (MIUR) by the PRIN program 2010/11 N. 2010MBJK5B.

References

Battipede, M., Ruotolo, R. and Surace, C. (2001), “Damage detection of plate-like structures”, *Key Eng. Mater*., **204**, 27-34.

Bayly, P.V., Johnson, E.E., Wolf, P.D., Smith,W. and Ideker, R. (1995), “Predicting patterns of epicardial potentials during ventricular fibrillation”, *IEEE T. Bio - Med. Eng*., **42**(9), 898-907.

Bentahar, M., El Guerjouma, R., Idijmarene, S. and Scalerandi, M. (2013), “Influence of noise on the threshold for detection of elastic nonlinearity”, *J. Appl. Phys*., **113**(4), 043516-043516-043511.

Cao, M. and Qiao, P. (2009), “Novel Laplacian scheme and multiresolution modal curvatures for structural damage identification”, *Mech. Syst. Signal Pr*., **23**(4), 1223-1242.

Cavalini Jr, A., Franco, V., Gonsalez, C., Lopes Jr., V. and De Melo, G. (2008), “Noise influence on damage detection through modal state observers methodology”, *Tema Tend Mater.Appl. Comput*., **9**(2), 195-204.

Cusumano, J., Sharkady, M. and Kimble, B. (1994), “Experimental measurements of dimensionality and spatial coherence in the dynamics of a flexible-beam impact oscillator”, *P. T. Roy. Soc. London. Series A: Phys. Eng. Sci*., **347**(1683), 421-438.

De Stefano, M., Gherlone, M., Mattone, M., Di Sciuva, M. and Worden, K. (2011), “Optimum sensor placement for impact location on multilayered composite structures using neural networks”, *Proceedings of the16th International Conference on Composite Structures ICCS 16*.

Doebling, S.W., Farrar, C.R. and Prime, M.B. (1998), “A summary review of vibration-based damage identification methods”, *Shock Vib*., **30**(2), 91-105.

Feeny, B. and Kappagantu, R. (1998), “On the physical interpretation of proper orthogonal modes in vibrations”, *J. Sound Vib*., **211**(4), 607-616.

Feeny, B. and Liang, Y. (2003), “Interpreting proper orthogonal modes of randomly excited vibration systems”, *J. Sound Vib*., **265**(5), 953-966.

Fitzsimons, P.M. and Rui, C. (1993), “Determining low dimensional models of distributed systems”, *Adv. Robust Nonlinear Control Syst*., 9-15.

Galvanetto, U., Monopoli, L., Surace, C. and Tassotti, A. (2007), “Experimental application of a damage localisation technique based on smoothed proper orthogonal modes”, *Key Eng. Mater*., **347**, 121-126.

Galvanetto, U., Surace, C. and Tassotti, A. (2008), “Structural damage detection based on proper orthogonal decomposition: experimental verification”, *AIAA J*.,**46**(7), 1624-1630.

Galvanetto, U. and Violaris, G. (2007), “Numerical investigation of a new damage detection method based on proper orthogonal decomposition”, *Mech. Syst. Signal Pr*., **21**(3), 1346-1361.

Ghajari, M., Sharif-Khodaei, Z., Aliabadi, M. and Apicella, A. (2013), “Identification of impact force for smart composite stiffened panels”, *Smart Mater. Struct*., **22**(8), 085014.

Ghajari, M., Sharif -Khodaei, Z. and Aliabadi, M. (2012), “Impact detection using artificial neural networks”, *Key Eng. Mater*., **488**, 767-770.

Gherlone, M., Mattone, M., Surace, C., Tassotti, A. and Tessler, A. (2005), “Novel vibration-based methods for detecting delamination damage in composite plate and shell laminates”, *Key Eng. Mater*., **293**, 289-296.

Giurgiutiu, V. (2008), *Structural health monitoring with piezoelectric wafer active sensors*, Academic Press.

Graham, M.D. and Kevrekidis, I.G. (1996), "Alternative approaches to the Karhunen-Loeve decomposition for model reduction and data analysis", *Comput. Chem. Eng*., **20**(5): 495-506.

Hamey, C.S., Lestari, W., Qiao, P. and Song, G. (2004), "Experimental damage identification of carbon/epoxy composite beams using curvature mode shapes", *Struct. Health Monit*., **3**(4), 333-353.

Hensman, J., Gherlone, M., Surace, C. and Di Sciuva, M. (2010), Probabilistic proper orthogonal decomposition, EWSHM.

Hensman, J., Surace, C. and Gherlone, M. (2011), "Detecting mode-shape discontinuities without differentiation–examining a Gaussian process approach", J. Physics: Conference Series, IOP Publishing.

Holmes, P., Lumley, J.L. and Berkooz, G. (1998), *Turbulence, coherent structures, dynamical systems and symmetry*, Cambridge University Press.

Kerschen, G., Golinval, J., Vakakis, A.F. and Bergman, L.A. (2005), "The method of proper orthogonal decomposition for dynamical characterization and order reduction of mechanical systems: an overview", *Nonlinear Dynam*., **41**(1), 147-169.

Kerschen, G. and Golinval, J.C. (2002), "Physical interpretation of the proper orthogonal modes using the singular value decomposition", *J. Sound Vib*., **249**(5), 849-865.

Limongelli, M. (2010), "Frequency response function interpolation for damage detection under changing environment", *Mech. Systems Signal Pr*., **24**(8), 2898-2913.

Limongelli, M. (2011), "The interpolation damage detection method for frames under seismic excitation", *J. Sound Vib*., **330**(22), 5474-5489.

Matworks (2012). Matlab 2012 documentation.

Qiao, P., Lu, K., Lestari, W. and Wang, J. (2007), "Curvature mode shape-based damage detection in composite laminated plates", *Compos. Struct*., **80**(3), 409-428.

Radzieński, M., Krawczuk, M. and Palacz, M. (2011), "Improvement of damage detection methods based on experimental modal parameters", *Mech. Syst. Signal Pr*., **25**(6), 2169-2190.

Rao, S.S. and Yap, F.F. (1995), *Mechanical vibrations*, Addison-Wesley Reading, MA.

Ratcliffe, C.P. (1997), "Damage detection using a modified Laplacian operator on mode shape data", *J. Sound Vib*., **204**(3), 505-517.

Ratcliffe, C.P. (2000), "A frequency and curvature based experimental method for locating damage in structures", *J. Vib. Acoust*., **122**(3), 324-329.

Ratcliffe, C.P. and Bagaria, W.J. (1998), "Vibration technique for locating delamination in a composite beam", *AIAA J*., **36**(6), 1074-1077.

Shane, C. and Jha, R. (2011), "Proper orthogonal decomposition based algorithm for detecting damage location and severity in composite beams", *Mech. Syst. Signal Pr*., **25**(3), 1062-1072.

Sharif-Khodaei, Z., Ghajari, M. and Aliabadi, M. (2012), "Determination of impact location on composite stiffened panels", *Smart Mater. Struct*., **21**(10), 105026.

Thiene, M., Galvanetto, U., Gherlone, M. and Aliabadi, M.H. (2014), "Application of Laplacian operators on noisy data to compute curvature with proper orthogonal decomposition", *Key Eng. Mater*., **577-578**, 241-244.

Thiene, M., Zaccariotto, M. and Galvanetto, U. (2013), "Application of proper orthogonal decomposition to damage detection in homogeneous plates and composite beams", *J. Eng. Mech. - ASCE*, **139**(11), 1539-1550.

Worden, K. and Staszewski, W. (2000), "Impact location and quantification on a composite panel using neural networks and a genetic algorithm", *Strain*, **36**(2), 61-68.

Wu, D. and Law, S. (2004), "Damage localization in plate structures from uniform load surface curvature", *J. Sound Vib*., **276**(1), 227-244.

Xiang, J., Matsumoto, T., Wang, Y. and Jiang, Z. (2012), "Detect damages in conical shells using curvature mode shape and wavelet finite element method", *Int. J. Mech. Sci*., **66**, 83-93.

Yoon, M., Heider, D., Gillespie, J., Ratcliffe, C. and Crane, R. (2005), "Local damage detection using the two-dimensional gapped smoothing method", *J. Sound Vib*., **279**(1), 119-139.

Zapico, J., Gonzalez, M. and Worden, K. (2003), "Damage assessment using neural networks", *Mech. Syst.*

Signal Pr., **17**(1), 119-125.

Zhang, Y., Lie, S.T. and Xiang, Z. (2012), “Damage detection method based on operating deflection shape curvature extracted from dynamic response of a passing vehicle”, *Mech. Syst. Signal Pr*., **35**(1-2), 238-254.

FC

Appendix 1

As already stated in Section 2 POD determines a series of modes, POMs, and energy coefficients, POVs, which are representative of the dynamics of the system under exam. As the frequency of the force tends to coincide with the first natural frequency of the system, the predominant POM becomesmore and more similar to the first linear natural mode (LNM) and its contribution to the final damage detection algorithm can be much more relevant than the variation of the other modes. Exploiting the similarity of POMs,the variations of LNMs with stiffness properties of a simple structure can provide a theoretical explanation of the relevance of the forcing frequency.

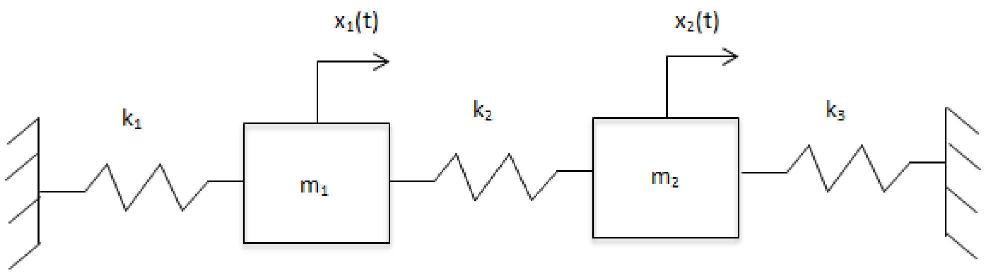

Fig. 20 Example of 2 DOF system

Consider the 2 degree of freedom (DOF) system shown in Fig. 20. Following the procedure describe in (Rao and Yap 1995), the equations of motion for a free vibration case are given by

$$\begin{aligned} \mathrm{m}_1\ddot{\mathrm{x}}_1(\mathrm{t})+(\mathrm{k}_1+\mathrm{k}_2)\mathrm{x}_1(\mathrm{t})-\mathrm{k}_2\mathrm{x}_2(\mathrm{t})=0 \\ \mathrm{m}_2\ddot{\mathrm{x}}_2(\mathrm{t})+(\mathrm{k}_2+\mathrm{k}_3)\mathrm{x}_2(\mathrm{t})-\mathrm{k}_2\mathrm{x}_1(\mathrm{t})=0 \end{aligned} \tag{13}$$

The solutions of the differential equations stated above can be expressed in the form

$$\begin{aligned} x_1(t)=X_1\cos(\omega t+\varphi) \\ x_2(t)=X_2\cos(\omega t+\varphi) \end{aligned} \tag{14}$$

Where X_1 and X_2 are constants that denote the maximum amplitude of the response, and φ is the phase angle. Substituting Eq. (14) in Eq. (13) and considering only the maximum amplitude response, as the equations must be satisfied for all the values of time t, it is possible to obtain

$$\begin{aligned} [-m_1\omega^2+(k_1+k_2)]X_1-k_2X_2=0 \\ [-m_2\omega^2+(k_2+k_3)]X_2-k_2X_1=0 \end{aligned} \tag{15}$$

For a non-trivial solution, the determinant of the coefficients must be zero. This implies that

$$(m_1 m_2)\omega^4 - [(k_1 + k_2)m_2 + (k_2 + k_3)m_1]\omega^2 + [(k_1 + k_2)(k_2 + k_3) - k_2{}^2] = 0 \tag{16}$$

At this point, since we want to evaluate the influence of k_2 on the mode shape, some simplifications are applied. In particular $m_1=m_2=m$ and $k_1=k_3=k$. the above equation reduces to

$$m^2\omega^4 - [(k + k_2)m + (k_2 + k)m]\omega^2 + [(k + k_2)(k_2 + k) - k_2{}^2] = 0 \tag{17}$$

The solutions of this equation are given by

$$\begin{aligned} &\omega_1{}^2, \omega_2{}^2 = \frac{1}{2}\left[\frac{2(k+k_2)m}{m^2}\right] \mp \frac{1}{2}\left[\left(\frac{2(k+k_2)m}{m^2}\right)^2 - 4\left(\frac{(k+k2)^2 - k_2{}^2}{m^2}\right)\right]^{\frac{1}{2}} \\ &\omega_1{}^2 = \frac{k}{m} \\ &\omega_2{}^2 = \frac{k+2k_2}{m} \end{aligned} \tag{18}$$

The ratios between the amplitudes of the response of the two masses are given by

$$\begin{aligned} r_1 &= \frac{X_2(\omega_1)}{X_1(\omega_1)} = \frac{-m\omega_1{}^2 + k + k_2}{k_2} = 1 \\ r_2 &= \frac{X_2(\omega_2)}{X_1(\omega_2)} = \frac{-m\omega_2{}^2 + k + k_2}{k_2} = -1 \end{aligned} \tag{19}$$

The above equations suggest that the two mode shapes, which are characteristic of the system under exam, are not sensitive to $k_2$nor k. This implies that a change in those parameters, due for example to damage, would not then be captured by the mode shapes, which could not therefore be used as damage indicator.

If instead $k_1=k_2$ the results are different, as it is possible to see from Fig. 21. The mode ratios change with a modification of k_3. Moreover the variation is different between the two modes**.**

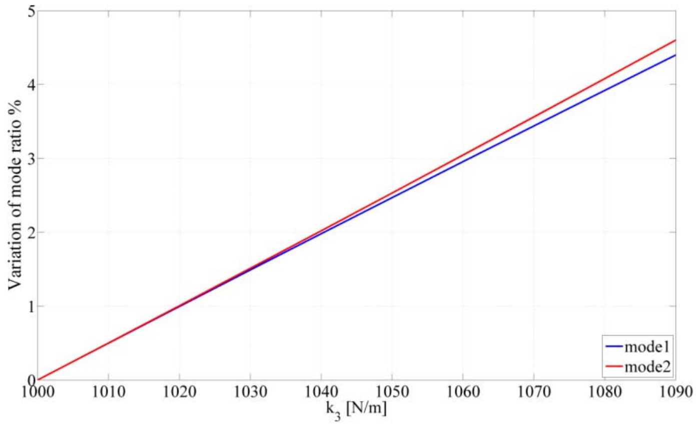

Fig. 21 Percentage variation of mode ratio with respect to k_3

The above considerations suggest that, depending on the mode shape chosen, the value of the damage index can be different. That is why the frequency of the load applied to compute the POD has a relevant role. Generally the first natural frequency of the system under exam is chosen; this is actually what was done in previous sections. In (Galvanetto and Violaris 2007) a more detailed analysis on the influence of the excitation frequency on a simple beam can be found.

Appendix 2

The number of points used to compute a modal shape of a system can considerably influence the result of the application of a damage detection technique. This is due to both a correct representation of the mode shape and a correct evaluation of its derivatives. Consider as a simple example the second mode shape of a cantilever beam of length 0.6 m. A good sampling of this shape can be obtained with 41 grid points with a spacing of 0.015 m. A bad sampling is obtained using only 9 points at a distance of 0.075 m. The results of the relevant shapes are presented in Fig. 22. It is clear that with the bad sampling some of the features of the mode shape can be not correctly predicted. These can include also possible damage.

The applications of derivative operations can exaggerate this problem. An estimation of the error in the calculation of the gradient with Eq. (7) is given by a Taylor series

$$u(x_i+h)=u(x_i)+h\left(\frac{\partial u}{\partial x}\right)_{x_i}+\frac{h^2}{2!}\left(\frac{\partial^2 u}{\partial x^2}\right)_{x_i}+\frac{h^3}{3!}\left(\frac{\partial^3 u}{\partial x^3}\right)_{x_i}+\cdots \tag{20}$$

This equation can be rearranged as:

$$\frac{u(x_i+h)-u(x_i)}{h}-\left(\frac{\partial u}{\partial x}\right)_{x_i}=\frac{h^2}{2!}\left(\frac{\partial^2 u}{\partial x^2}\right)_{x_i}+\frac{h^3}{3!}\left(\frac{\partial^3 u}{\partial x^3}\right)_{x_i}+\cdots \tag{21}$$

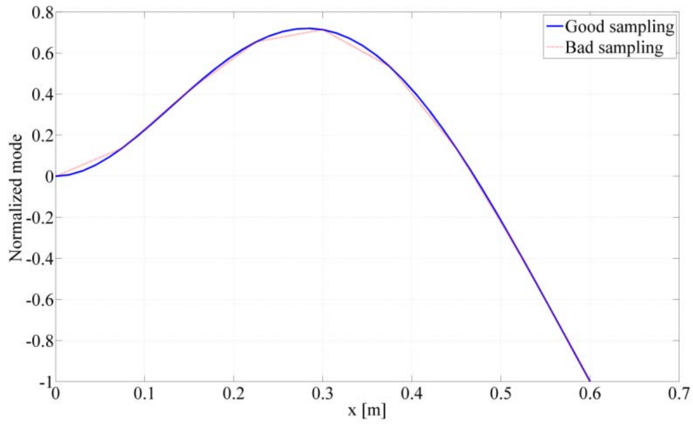

Fig. 22 Examples of good and bad sampling in the evaluation of the mode shape

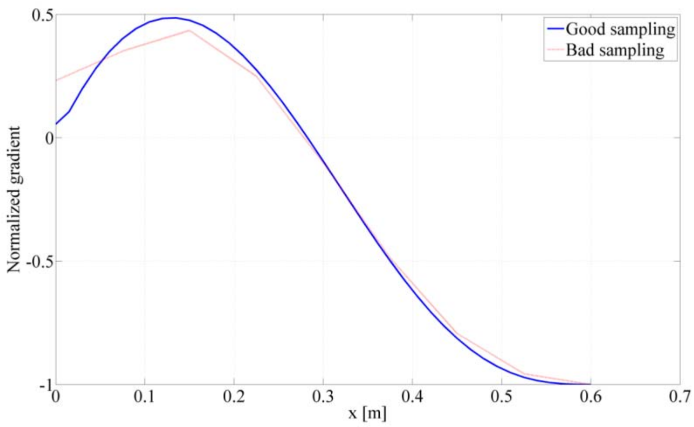

Fig. 23 Example of good and bad sampling in the evaluation of the gradient of the mode shape

The second term in Eq. (21) is the truncation error. When h is small enough, the left hand of Eq. (21) is a correct representation of the gradient of a function; otherwise the truncation error becomes relevant. Similar considerations can be derived for the curvature. An example of the gradient of the considered mode is given in Fig. 23.